ACS Photonics

Article

Cite This: ACS Photonics 2018, 5, 1303−1309

Room-Temperature Lasing Action in GaN Quantum Wells in the Infrared 1.5 μm Region

V. X. Ho,[†] T. M. Al tahtamouni,[‡] H. X. Jiang,[§] J. Y. Lin,[§] J. M. Zavada,[∥] and N. Q. Vinh*[,†]

[†]Department of Physics and Center for Soft Matter and Biological Physics, Virginia Tech, Blacksburg, Virginia 24061, United States

[‡]Materials Science and Technology Program, College of Arts and Sciences, Qatar University, Doha 2713, Qatar

[§]Department of Electrical and Computer Engineering, Texas Tech University, Lubbock, Texas 79409, United States

[∥]Department of Electrical and Computer Engineering, New York University, Brooklyn, New York 11201, United States

Supporting Information

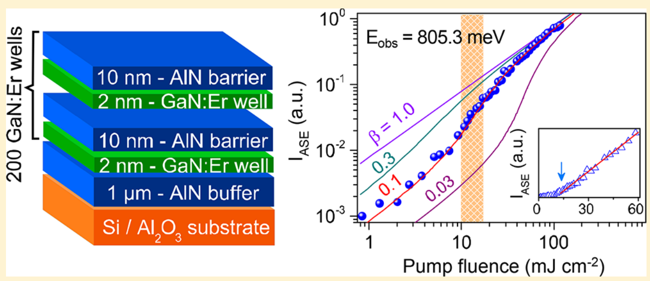

ABSTRACT: Large-scale optoelectronics integration is strongly limited by the lack of efficient light sources, which could be integrated with the silicon complementary metal-oxide-semiconductor (CMOS) technology. Persistent efforts continue to achieve efficient light emission from silicon in extending the silicon technology into fully integrated optoelectronic circuits. Here, we report the realization of room-temperature stimulated emission in the technologically crucial 1.5 μm wavelength range from Er-doped GaN multiple-quantum wells on silicon and sapphire. Employing the well-acknowledged variable stripe technique, we have demonstrated an optical gain up to 170 cm^{-1} in the multiple-quantum well structures. The observation of the stimulated emission is accompanied by the characteristic threshold behavior of emission intensity as a function of pump fluence, spectral line width narrowing, and excitation length. The demonstration of room-temperature lasing at the minimum loss window of optical fibers and in the eye-safe wavelength region of 1.5 μm are highly sought after for use in many applications including defense, industrial processing, communication, medicine, spectroscopy, and imaging. As the synthesis of Er-doped GaN epitaxial layers on silicon and sapphire has been successfully demonstrated, the results laid the foundation for achieving hybrid GaN-Si lasers, providing a new pathway toward full photonic integration for silicon optoelectronics.

KEYWORDS: *silicon, GaN, quantum wells, lasing, infrared laser, rare earth*

Driven by the strong need for cheap and integrable Si-based optoelectronic devices for a wide range of applications, continuing endeavors have been made to develop structures for light emission, modulation, and detection in this material system. Recent breakthroughs, including the demonstration of a high-speed optical modulator in Si,[1,2] photodetectors,[3] and waveguides,[4] have brought the concept of transition from electrical to optical interconnects closer to realization. However, the base for silicon photonics, namely, a group IV laser source, still has to be developed. Due to the relatively small and indirect band gap, silicon is a poor light emitter. Nevertheless, lasing devices based on Si have been demonstrated including Si-based impurity lasers,[5] a Raman laser,[6] Si nanocrystals,[7] nanopatterned crystalline Si,[8] GeSn alloy on Si,[9] Ge dots in Si,[10,11] and InGaAs/GaAs nanolasers grown on Si.[12] However, these prototype devices essentially lack the advantages associated with the silicon system by requiring an external pump laser source or function only at low temperatures. While room-temperature luminescence has been realized,[7,13] population inversion and optical gain have been under discussion and fundamental problems remain.

The incorporation of rare earth elements into semiconductor hosts gives rise to sharp, atomic-like, and temperature-independent emission lines under either optical or electrical excitation.[14−18] Er ions with intra-4*f* shell transitions from its first excited state ($^4I_{13/2}$) to the ground state ($^4I_{15/2}$) produce 1.5 μm emission which falls within the minimum loss window of optical fibers for optical communications and in the eye-safe wavelength region. Lasers operating around 1.5 μm are highly sought-after for use in defense, industrial processing, medicine, spectroscopy, imaging, and various other applications where the laser beam is expected to travel long distances in free space. With a tremendous effort, 1.5 μm emission from Er-doped narrow-bandgap semiconductors including Si and GaAs has a low efficiency at room-temperature due to the strong thermal quenching effect.[15,19]

■ RESULTS AND DISCUSSION

Recently, we have successfully synthesized GaN:Er epilayers on Si(001)[20,21] and c-plane sapphire[22] substrates by metal organic

Received: October 23, 2017
Published: February 22, 2018

DOI: 10.1021/acsphotonics.7b01253
ACS Photonics 2018, 5, 1303−1309

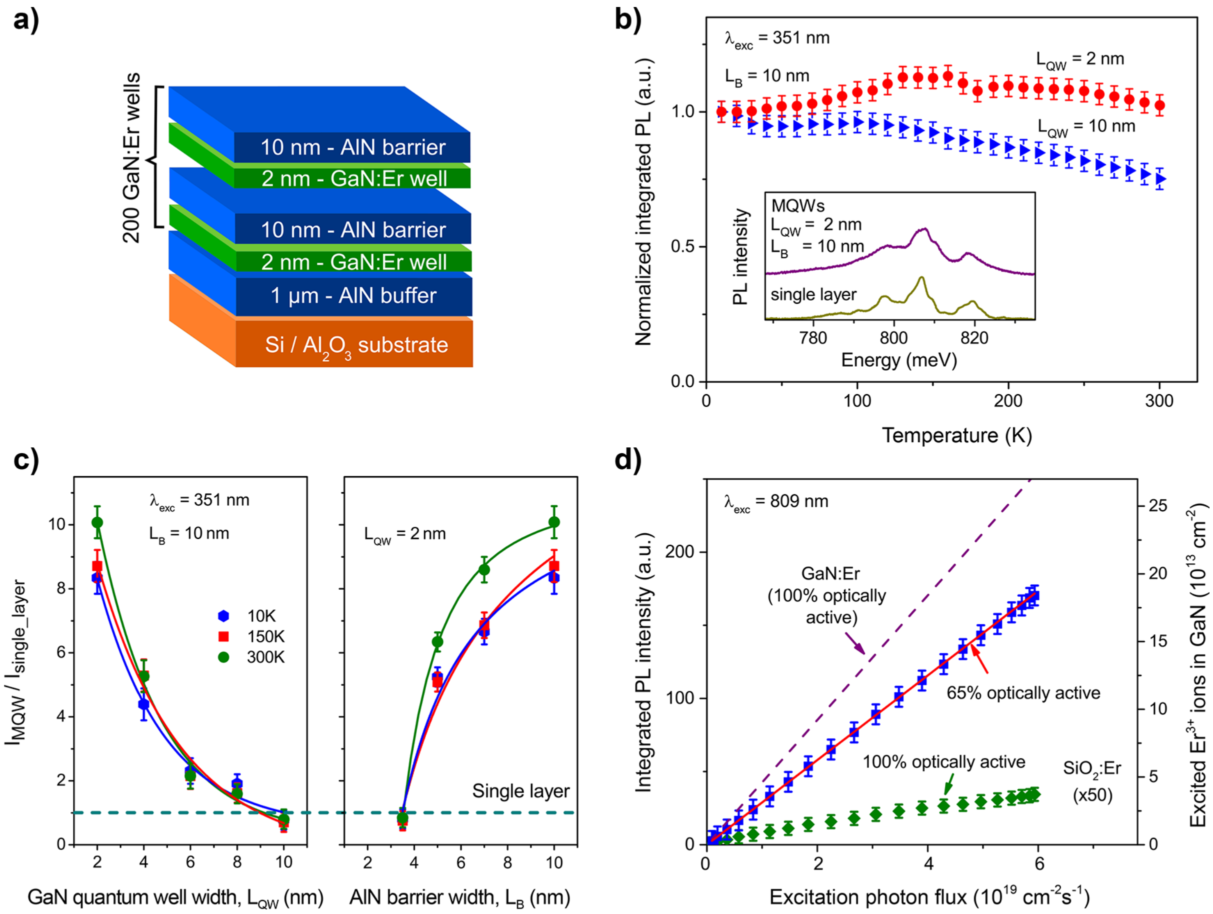

Figure 1. Schematic of Er doped GaN/AlN MQWs and PL intensity data at 1.5 μm. (a) A 200-period MQWs:Er sample with the GaN quantum well width, L_{QW}, of 2 nm and the AlN barrier thickness, L_B, of 10 nm. (b) The temperature dependence of PL intensity for two samples with the same the barrier thickness, L_B = 10 nm, but two different quantum well widths, L_{QW} = 2 and 10 nm, under the band-to-band excitation, λ_{exc} = 351 nm. Inset: a typical PL spectrum from MQWs:Er materials and a single GaN:Er epilayer collected from the surface showing the spontaneous emission process. (c) Integrated PL intensity ratio of MQWs:Er samples to a single GaN:Er epilayer at 1.5 μm as a function of the quantum well width, L_{QW} (left) and the barrier thickness, L_B (right), measured at different temperatures from 10 K to room-temperature under the over bandgap excitation. The maximum PL intensity was obtained with a MQWs:Er sample having L_{QW} = 2 nm and L_B = 10 nm. (d) Comparison of the integrated PL intensity of Er^{3+} ions in MQWs with the reference SiO_2:Er sample under the resonant ($^4I_{15/2} \rightarrow {}^4I_{9/2}$) excitation, λ_{exc} = 809 nm. Measurements indicated that ~65% of Er^{3+} ions are optically active centers in the MQWs:Er sample with L_{QW} = 2 nm and L_B = 10 nm.

chemical vapor deposition (MOCVD) with excellent material qualities. The above host bandgap[20−23] and electroluminescence[24] excitation of Er optical centers produced predominant light emission at 1.5 μm range. In order to overcome the challenges of growth of III-nitrides on Si(100) substrate due to the different crystalline structures between GaN and Si, we have employed selective area growth and epitaxial lateral overgrowth techniques to prepare GaN/AlN/Si(100) templates.[20] The X-ray diffraction and photoluminescence (PL) measurements indicated that GaN:Er epilayers grown on Si and sapphire have high crystallinity, without second phase formation,[20−22] and exhibit a strong room-temperature emission at 1.5 μm with a low degree of thermal quenching.[22,23] In this work, a set of 200-period Er-doped GaN/AlN multiple quantum wells (MQWs:Er) produced a significant improvement of the quantum efficiency of the 1.5 μm emission via carrier quantum confinement and strain engineering[25] (see schematic in Figure 1a). The growth process was started with AlN buffer and template layers and then followed by the growth of the MQWs:Er. The structure consists of alternating layers of Er doped GaN quantum wells and undoped AlN barriers (see Methods and Supporting Information). A detailed description of the growth process and epilayer structure has been reported previously.[25]

Typical room-temperature PL spectra from the MQWs:Er samples and a single GaN:Er epilayer show a broad spectral feature[25] around 1.5 μm under the band-to-band excitation using an Ar laser at 351 nm (Figure 1 b, inset). The PL spectrum was collected from the surface of the sample, which is the spontaneous emission of light from Er optical centers in MQWs. As previously reported, the full-width at half-maximum (fwhm) of the 1.5 μm emission at room-temperature is 50 nm for a single GaN:Er epilayer[22,23] and 60 nm for MQWs:Er materials.[25] The broadening of the emission in MQWs is due to the fluctuation of the GaN quantum well width and the local atomic structures around Er optical centers. This is especially a factor for Er optical centers located close to the quantum well/barrier interfaces.

The emission intensity from the MQWs:Er structure is an order of magnitude higher than that of a single GaN:Er epilayer with the same Er doping active layer thickness and concentration under the over bandgap excitation, λ_{exc} = 351 nm. The strong quantum confinement effects on the Er emission have been studied for different values of quantum

DOI: 10.1021/acsphotonics.7b01253
ACS Photonics 2018, 5, 1303−1309

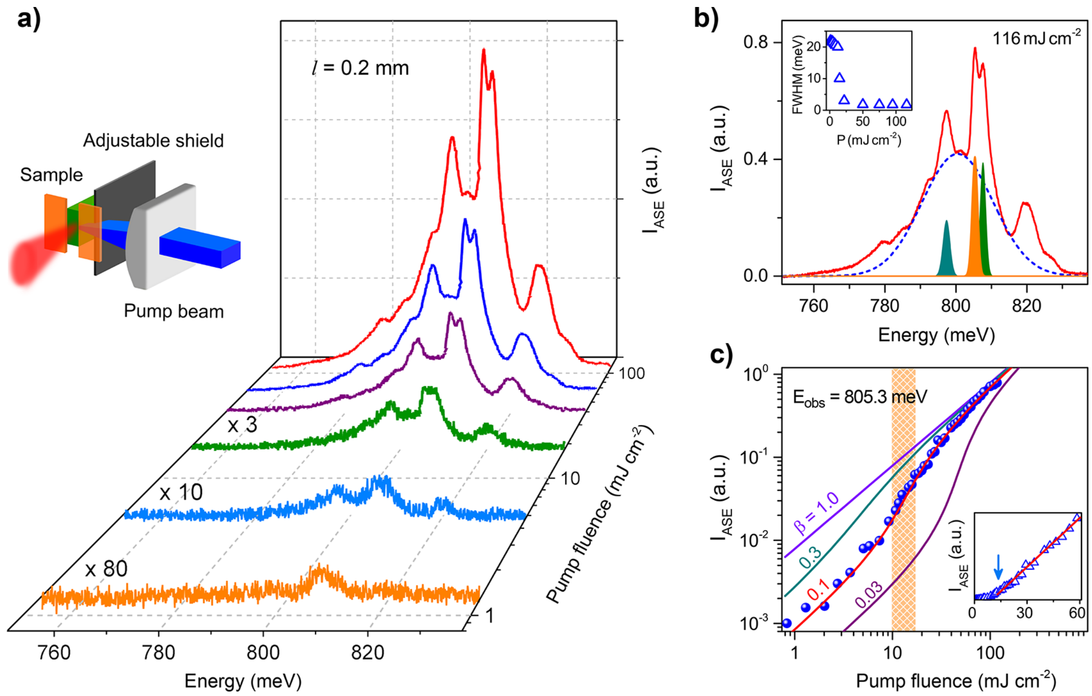

Figure 2. Amplified spontaneous emission, at room-temperature, from the MQWs:Er sample with L_{QW} = 2 nm and L_B = 10 nm using an Ar laser, λ_{exc} = 351 nm, for the band-to-band excitation. (a) Pump-fluence dependent PL spectra obtained with a 8 μm wide and 0.2 mm long pump excitation. At low excitation pump fluence, the emission is broad with the fwhm of 30 meV. When the pump fluence is high enough for the optical layer to have net gain, the spontaneously emitted photons are exponentially amplified by stimulated emission and the spectral peaks become narrower. Inset: Schematic of experimental configuration for edge-emission and variable excitation length measurements. (b) PL spectrum at room-temperature with a pump fluence of 116 mJ cm^{-2} and an excitation length of 0.2 mm. The spectrum was deconvolved into six Gaussian peaks. The most prominent modes show a fwhm of 1.60 ± 0.25 meV. Inset: The fwhm of the Gaussian peaks decreases with increasing the pump fluence. (c) L-L data on a log–log scale showing the dependence of the edge-emission intensity for PL peak at 805.3 meV on the pump fluence. The excitation length was 0.2 mm and the data were fitted using the S-curve model. Inset: The edge-emission intensity showing linear behavior below threshold and superlinear increase at higher pump fluence.

wells and barriers. In Figure 1c, the integrated PL intensity ratio of MQWs:Er samples, I_{MQW}, to a single GaN:Er epilayer, I_{single_layer}, at 1.5 μm is shown as a function of the GaN quantum well width, L_{QW}, (left) and the AlN barrier thickness, L_B, (right), measured at temperatures from 10 K to room-temperature. As shown in the Figure 1c (left) for MQWs:Er samples with L_B = 10 nm, the integrated PL intensity, I_{MQW}, increases significantly when L_{QW} was reduced from 10 to 2 nm. In these measurements, I_{MQW} is normalized to the integrated PL intensity of the single GaN:Er epilayer, I_{single_layer}, with the same total Er doping active layer thickness and concentration. When the quantum well width, L_{QW}, is larger than 10 nm, I_{MQW} is approximately equal to I_{single_layer} (the horizontal dashed lines in Figure 1c). A decreasing of the quantum well width provides a strong quantum confinement effect of carriers around Er ions, thus improves the quantum efficiency of the 1.5 μm emission from Er ions in GaN. When the quantum well width is smaller than the free exciton Bohr radius of 2.8 nm in GaN,[26] the built-in electrical fields due to the lattice mismatch between GaN/AlN produce further the strong quantum confinement effect for excitons, resulting in an efficient energy transfer from excitons to Er optical centers. The highest integrated PL intensity has been obtained for L_{QW} = 2 nm (Figure 1c, left). For MQWs:Er samples with L_{QW} = 2 nm, the integrated PL intensity, I_{MQW}, is enhanced by more than 1 order of magnitude over that of the single GaN:Er epilayer via the variation of the AlN barrier thickness, L_B (Figure 1c, right). When the L_B is larger than the exciton Bohr radius in GaN, electron wave functions are localized at the quantum well. A large AlN barrier thickness provides an increased probability of capturing excitons by Er optical centers, leading to a higher excitation efficiency of Er^{3+} ions. We have obtained the maximum I_{MQW} at 1.5 μm when the AlN L_B is above 10 nm.

In order to evaluate the thermal quenching effect of the 1.5 μm emission, we have performed the temperature dependence of the integrated PL intensity of MQWs:Er samples under the band-to-band excitation, λ_{exc} = 351 nm. The PL experiments were carried out in a variable temperature closed-cycle optical cryostat (Janis) providing a temperature range from 10 to 300 K. The integrated PL intensity of Er in the single GaN:Er epilayer, I_{single_layer}, is reduced by about 20% from 10 K to room-temperature (Figure S3a, Supporting Information).[23] The integrated PL intensity of Er in MQWs:Er samples, I_{MQW}, with quantum well width larger than the exciton Bohr radius in GaN and the AlN barrier thickness thinner than 10 nm follow the same temperature dependence behaviors as the single GaN:Er epilayer, I_{single_layer} (Figure 1b). However, when the thicknesses of the quantum wells and barriers are close to the optimal parameters (L_{QW} = 2 nm, L_B = 10 nm), the temperature dependence of PL intensity is quite different. The highest value of I_{MQW} occurs at 150 K and the values of I_{MQW} at 10 K and room-temperature are comparable (Figure 1b). When the temperature increases, the mobility of carriers in GaN increases significantly and reaches a maximum around 130 K.[27,28] The increasing of the carrier mobility provides higher efficiency for the energy transfer from GaN quantum wells to

DOI: 10.1021/acsphotonics.7b01253
ACS Photonics 2018, 5, 1303−1309

Er ions, resulting in the stronger PL emission intensity. The contamination of Al in MQW structures can also provide a factor that affects the thermal property of the PL intensity of Er ions. We have further conducted the temperature dependence of the PL emission intensity for different MQW structures (see Supporting Information). In this work, we compare the PL intensity from MQWs:Er samples with the optimal structure, that is, L_{QW} = 2 nm and L_B = 10 nm, and a GaN:Er single layer.

The percentage of Er ions that emit photons at 1.5 μm is a crucially important parameter for potential applications of Er-doped GaN since it determines the PL intensity as well as population inversion. An estimate of the number of emitting Er optical centers can be made by comparing the PL intensity of the MQWs:Er sample with that of a SiO_2:Er reference sample with the same shape and under the same experimental conditions. In order to avoid the quantum confinement effect for excitons and carriers, the experiment has been performed at room-temperature under the resonant excitation $^4I_{15/2} \rightarrow {}^4I_{9/2}$ transition using the Ti:sapphire laser at 809 nm. Note that under the band-to-band excitation several Er centers are excited, including dark, bright centers. We have observed two kinds of optical centers in the single GaN:Er epilayer, including the defect-related and isolated Er optical centers.[23] The PL from defect-related Er optical centers can be observed under the band-to-band excitation and at the sample temperature below 150 K. The isolated Er optical centers can be excited by both resonant and band-to-band excitation. Thus, it is the correct way to employ the resonant excitation for this estimation. The time-integrated PL intensity of these samples are collected as a function of applied photon fluxes (Figure 1d). By comparing the PL from Er ions in the MQWs:Er sample with the reference sample of Er-doped SiO_2, we have estimated that the fraction of Er ions that emits photon at 1.5 μm is approximately 65% (Supporting Information). Using the same method, we found that a fraction of ~68% of Er ions in the single GaN:Er layer is optically active.[29] This achievement of the high percentage of Er ions that emit photons at 1.5 μm represents a significant step in realization of GaN:Er as an optical gain medium.

The edge-emission from optically pumped MQWs:Er sample under the band-to-band excitation provides evidence of room-temperature lasing from Er optical centers in the MQW structure (Figure 2a, inset). In order to achieve lasing from the MQWs:Er sample, both edges of the sample were polished to obtain a cavity. The edge-emission spectra from Er optical centers are different at different pump fluence near threshold (Figure 2a). In the measurements we have employed a long excitation area with 8.0 ± 0.3 μm width and 200 ± 0.5 μm length (Figure 2a, inset and Methods). The photon fluence of the Ar laser was varied from 0.05 to 120 mJ cm^{-2}. At low excitation pump fluence (P < 15 mJ cm^{-2}), the emission at 1.5 μm shows a broad spectrum with the fwhm of 60 nm (~30 meV) that corresponds to the spontaneous emission.[25] The broad PL spectrum is similar to those of Er ions incorporated in insulators including SiO_2 at room-temperature. When the pump fluence is high enough (P > 15 mJ cm^{-2}) for the MQWs:Er sample to obtain a net optical gain, the spontaneously emitted photons are exponentially amplified by stimulated emission as they travel through the waveguide in the active medium, leading to a superlinear increase in emission. Since the gain is maximum near the peak of the spontaneous emission spectrum, the spectrum exhibits "gain narrowing".[30,31] Consequently, an intense beam with spectral narrowing is emitted from the edge of the sample. The amplified spontaneous emission occurs at the wavelength where the spontaneous emission spectrum is strongest. The PL spectra at high excitation pump fluence indicate a number of strong and narrow PL lines. This is the signature of optical amplification of the spontaneous emission from Er optical centers around 1.5 μm in the MQW structure (Figure 2b). We focus to analyze the strongest PL lines at 797.31, 805.30, and 807.55 meV. A deconvolution of the PL spectrum into different Gaussian components is also shown. When the pump fluencies were above 15 mJ cm^{-2}, the fwhm of the spectrum dropped to 1.60 ± 0.25 meV (Figure 2b, inset). The PL intensity evolution of narrow peaks indicates a clear threshold transition from subthreshold to linear evolution and ultimately reaches saturation at high pump-fluence (Figure 2b).

A closer examination of this threshold behavior of the PL intensity emitted from the edge of the sample shows the typical superlinear (exponential) to linear transition, indicating the classical spontaneous-to-stimulated emission transition widely observed in semiconductor lasers.[32] Figure 2c shows the light-in-light-out (L-L) data that is the dependence of the amplified spontaneous emission on the pump fluence for the PL peak at 805.3 meV (1539.61 nm) with the excitation length of 0.2 mm. Below the threshold, the PL dependence is linear and a superlinear increase in emission intensity with pump fluence has been observed. Subsequently, stimulated emission dominates and the PL intensity evolution becomes linear (Figure 2c, inset). Fitting the L-L data in the log−log plot to the S-curve model,[32,33] a lasing threshold of P_{th} ~ 15 mJ cm^{-2} has been determined (Figure 2c), with the spontaneous emission coupling factor, β, of 0.1. The L-L curves for different β values are also plotted for comparison, clearly showing the distinct position of the lasing threshold. Additional representative L-L plots of MQWs:Er lasing under optical pumping with different excitation lengths can be found in Supporting Information. Above the threshold for amplified spontaneous emission, most of the excitation was stimulated to emit light into waveguide modes, leading to a large fraction of the light emerged from the edge.[30,34]

Together with the threshold behavior, we have observed the shortening of the lifetime of Er emission in the MQW structure. A typical lifetime of Er spontaneous emission in the MQW structures with the pump fluence below the threshold is around 2.5 ms (red curve, Figure S4, Supporting Information). Under a high pump fluence (above the threshold), the lifetime of Er emission shows a shortening with a dynamics <10 μs (blue curve, Figure S4, Supporting Information). The value is limited by the time-constant of our time-resolved photoluminescence setup. We have integrated the PL intensity for the fast and slow components. The PL spectrum for the fast component shows narrowing features as indicated in the Figure 2a at high pump fluence. The PL spectrum for the slow component is similar to the spectrum at low pump fluence. The PL intensity of the slow component can be originated from surface emission of the sample.

We have employed the well-known variable excitation length method to determine the gain coefficient from the evolution of the peak-emission intensity (Methods).[35] The sample was optically excited by the argon laser providing the band-to-band excitation in a stripe geometry. The amplified spontaneous emission signal, I_{ASE}, was collected as a function of the illuminated length or the excitation length, l, from the edge of the sample. As a result of stimulated emission, the spontaneous

DOI: 10.1021/acsphotonics.7b01253
ACS Photonics 2018, 5, 1303−1309

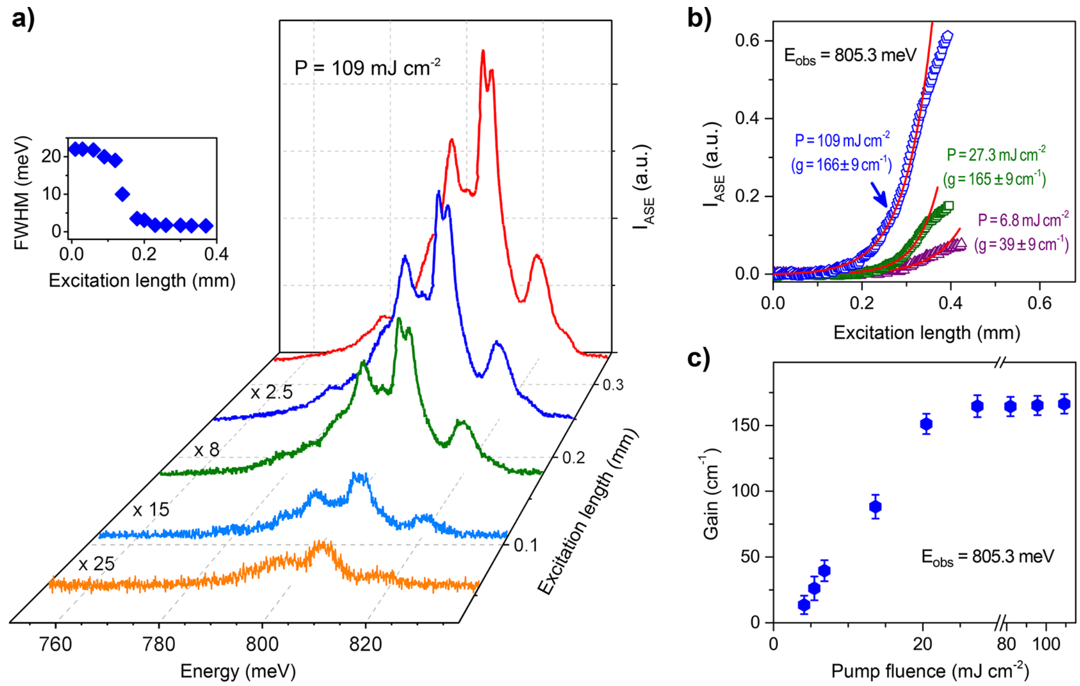

Figure 3. Optical gain determination via the variable stripe length method. (a) Edge-emission PL spectra from the MQWs:Er sample with L_{QW} = 2 nm and L_B = 10 nm as a function of the excitation length at a pump fluence of 109 mJ cm^{-2}. The PL spectra become sharper at higher pump fluence due to the amplified spontaneous emission. The narrowing of the edge-emission spectral peaks provides evidence of lasing in the MQWs:Er sample at room-temperature. Inset: The reduction of the fwhm of the deconvoluted Gaussian peaks with increasing the excitation lengths. (b) Dependence of the amplified spontaneous emission intensity, for the PL peak at 805.3 meV, on excitation length. The modal gain of the MQWs:Er sample was determined by using eq 1 to the data. (c) The net gain of the sample at 805.3 meV as a function of the pump fluence.

emitted light is amplified as it passes through the excited volume to the edge of the sample. Assuming a one-dimensional amplification model, the modal gain, g_{mod}, can be extracted from the amplified spontaneous emission intensity and the excitation length:[35]

$$I_{ASE}(l) = \frac{A \times I_{SPONT}}{g_{mod}}(e^{g_{mod}l} - 1) \tag{1}$$

where I_{SPONT} is the spontaneous emission intensity per unit length and A is the cross-section area of the excited volume, and the modal gain is the gain minus the loss of the material.

When the excitation length was varied, the emission spectral peaks became narrower as the excitation length was increased, and the output intensity grew exponentially. Figure 3a presents the PL spectra with an optical excitation of 109 mJ cm^{-2} for different excitation lengths. The observation of an exponential increase in the intensity and a substantial decrease in spectral line width (Figure 3a, inset) of light emitted as the excitation length is varied is a direct indication of the optical gain. Figure 3b shows the output intensity at the observation peak at 805.3 meV as a function of excitation length at three different pump fluence. In each case, the data can be fitted to eq 1. The net gain of the waveguide was measured as a function of the pump intensity (Figure 3c). At higher pump fluence, the output intensity increased exponentially with excitation lengths less than 0.42 mm, and then leveled off at longer excitation lengths. This behavior can be attributed to gain saturation, which occurs when the light traveling in the waveguide becomes so intense that it depletes a substantial fraction of the excited centers and reduces the gain coefficient. We limited the gain analysis to pump fluence <150 mJ cm^{-2} and excitation lengths <0.42 mm.

In conclusion, our investigations provide conclusive evidence of light amplification and stimulated emission in MQWs:Er samples. In the past, this formidable goal was unsuccessfully attempted by Er doping of crystalline Si, and later of SiO_2 sensitized with Si nanocrystals. Here we have demonstrated the realization of this long-sought goal of Si photonics in state-of-the-art GaN MQW structures grown on-Si and GaN, demonstrating for the first time the added value provided by merging of these two most important semiconductor materials – Si for standard electronics and photovoltaics and GaN for power electronics, photonics and automotive applications.

METHODS

Sample Fabrication. Er-doped GaN/AlN MQWs (MQWs:Er) were grown by MOCVD. The aluminum source was trimethylaluminum (TMA), the gallium source was trimethylgallium (TMGa), and the nitrogen source was ammonia (NH_3). Trisisopropylcyclopentadienylerbium (TRIPEr) was used as a precursor for in situ Er doping. The growth started with a thin (30 nm) AlN buffer layer (buffer 1) grown at 950 °C and 30 mbar followed by a second 100 nm AlN buffer layer (buffer 2) at 1100 °C grown at 30 mbar, and a 1.0 μm AlN template grown at 1325 °C and 30 mbar. It was then followed by the growth of the MQWs:Er structure of Er-doped GaN quantum wells and undoped AlN barrier layers. The growth temperature and pressure were 1000 °C and 30 mbar.

PL Intensity Measurement. The PL spectra were collected with a high resolution Horiba iHR550 spectrometer equipped with a 900 grooves/mm grating blazed at 1.5 μm and detected by a high sensitivity liquid nitrogen InGaAs DSS-IGA detector. The resolution of PL spectrum is 0.05 nm. The PL

DOI: 10.1021/acsphotonics.7b01253
ACS Photonics 2018, 5, 1303−1309

experiments were carried out in a variable temperature closed-cycle optical cryostat (Janis) within the temperature range from 10 to 300 K. We have employed resonant and nonresonant excitation to investigate optical properties from the MQWs:Er structures.[23] An Argon laser emitting light at 351 nm (3.531 eV) was employed for the nonresonant (band-to-band) excitation of MQWs:Er materials. The PL spectra under the resonant excitation from $^4I_{15/2} \rightarrow {}^4I_{9/2}$ of Er^{3+} in GaN were obtained using a tunable wavelength Ti:sapphire laser around 809 nm (1.533 eV).[23]

Edge-Emission Measurements. The pump laser was magnified and then focused onto the sample's top surface using a cylindrical lens with f = 7.5 cm (Figure 2b, inset). Only the central part of the laterally unfocused laser spot was used to excite the sample so that the pump fluence was uniform across the entire excited area. The excitation area was measured to be a long stripe of 8.0 ± 0.3 μm width exciting the entire sample length of 1000 ± 0.5 μm. We used a two-dimensional linear stage to scan our UV photodetector at the focal position of the laser to verify that within experimental conditions the laser pump fluence on the sample surface was constant and independent of the length. No influence of diffraction effects on the uniformity of the pump laser were detected. An aperture was used to ensure that none of the light, which has passed out of the excited volume before reaching the edge of the sample, was detected. The edge-emission was collected using a set of two lenses f = 10 and 24 cm, with a diameter of 5 cm, and focused onto the entrance slit of the high resolution spectrometer through a long-pass filter blocking all background light with a wavelength shorter than 950 nm. All the edge-emission measurements were done at room-temperature. The photon fluence on the sample was varied from 0.05 to 500 mJ cm^{-2}.

Gain Measurements. Net optical gain of the MQWs:Er sample with optimized structural parameters (i.e., GaN L_{QW} = 2 nm and AlN L_B = 10 nm) was measured using variable excitation length method. In the same edge-emission measurement configuration, a mobile blade was mounted on an ultraprecise linear translation stage (relative accuracy of 80 nm). The edge-emission was collected and focused onto the entrance slit of the spectrometer as described. The measured gain coefficients show a fluctuation of within 5% for different distances between the sample's top surface and the mobile blade, suggesting that diffraction effects can be safely disregarded.

ASSOCIATED CONTENT

Supporting Information

The Supporting Information is available free of charge on the ACS Publications website at DOI: 10.1021/acsphotonics.7b01253.

> Details of the fabrication procedure of MOCVD growth of Er-doped multiple quantum wells, temperature dependence of MQWs:Er samples, optical activity determination, and rate equation analysis (PDF).

AUTHOR INFORMATION

Corresponding Author

*E-mail: vinh@vt.edu.

ORCID

V. X. Ho: 0000-0001-5413-9030

N. Q. Vinh: 0000-0002-3071-1722

Author Contributions

V.X.H. performed the optical and lasing experiments supervised by N.Q.V.; N.Q.V., H.X.J., J.Y.L., and J.M.Z. designed the research program; H.X.J., J.Y.L., and T.M.A. were in charge of MOCVD growth of Er-doped GaN epilayers and MQW samples; and N.Q.V., V.X.H., J.Y.L., and J.M.Z. wrote the paper.

Notes

The authors declare no competing financial interest.

ACKNOWLEDGMENTS

N.Q.V. acknowledges the support from NSF (ECCS-1358564). The materials growth effort at TTU was supported by JTO/ARO (W911NF-12-1-0330).

REFERENCES

(1) Liu, A. S.; Jones, R.; Liao, L.; Samara-Rubio, D.; Rubin, D.; Cohen, O.; Nicolaescu, R.; Paniccia, M. A high-speed silicon optical modulator based on a metal-oxide-semiconductor capacitor. *Nature* **2004**, *427* (6975), 615.

(2) Xu, Q. F.; Schmidt, B.; Pradhan, S.; Lipson, M. Micrometre-scale silicon electro-optic modulator. *Nature* **2005**, *435* (7040), 325.

(3) Assefa, S.; Xia, F. N. A.; Vlasov, Y. A. Reinventing germanium avalanche photodetector for nanophotonic on-chip optical interconnects. *Nature* **2010**, *464* (7285), 80.

(4) Xia, F. N.; Sekaric, L.; Vlasov, Y. Ultracompact optical buffers on a silicon chip. *Nat. Photonics* **2007**, *1* (1), 65.

(5) Pavlov, S. G.; Zhukavin, R. K.; Orlova, E. E.; Shastin, V. N.; Kirsanov, A. V.; Hubers, H. W.; Auen, K.; Riemann, H. Stimulated emission from donor transitions in silicon. *Phys. Rev. Lett.* **2000**, *84* (22), 5220.

(6) Rong, H. S.; Jones, R.; Liu, A. S.; Cohen, O.; Hak, D.; Fang, A.; Paniccia, M. A continuous-wave Raman silicon laser. *Nature* **2005**, *433* (7027), 725.

(7) Pavesi, L.; Dal Negro, L.; Mazzoleni, C.; Franzo, G.; Priolo, F. Optical gain in silicon nanocrystals. *Nature* **2000**, *408* (6811), 440.

(8) Cloutier, S. G.; Kossyrev, P. A.; Xu, J. Optical gain and stimulated emission in periodic nanopatterned crystalline silicon. *Nat. Mater.* **2005**, *4* (12), 887.

(9) Wirths, S.; Geiger, R.; von den Driesch, N.; Mussler, G.; Stoica, T.; Mantl, S.; Ikonic, Z.; Luysberg, M.; Chiussi, S.; Hartmann, J. M.; Sigg, H.; Faist, J.; Buca, D.; Grutzmacher, D. Lasing in direct-bandgap GeSn alloy grown on Si. *Nat. Photonics* **2015**, *9* (2), 88.

(10) Grydlik, M.; Hackl, F.; Groiss, H.; Glaser, M.; Halilovic, A.; Fromherz, T.; Jantsch, W.; Schaffler, F.; Brehm, M. Lasing from Glassy Ge Quantum Dots in Crystalline Si. *ACS Photonics* **2016**, *3* (2), 298−303.

(11) Grydlik, M.; Lusk, M. T.; Hackl, F.; Polimeni, A.; Fromherz, T.; Jantsch, W.; Schaffler, F.; Brehm, M. Laser Level Scheme of Self-Interstitials in Epitaxial Ge Dots Encapsulated in Si. *Nano Lett.* **2016**, *16* (11), 6802−6807.

(12) Chen, R.; Tran, T. T. D.; Ng, K. W.; Ko, W. S.; Chuang, L. C.; Sedgwick, F. G.; Chang-Hasnain, C. Nanolasers grown on silicon. *Nat. Photonics* **2011**, *5* (3), 170.

(13) Sun, Y.; Zhou, K.; Sun, Q.; Liu, J. P.; Feng, M. X.; Li, Z. C.; Zhou, Y.; Zhang, L. Q.; Li, D. Y.; Zhang, S. M.; Ikeda, M.; Liu, S.; Yang, H. Room-temperature continuous-wave electrically injected InGaN-based laser directly grown on Si. *Nat. Photonics* **2016**, *10* (9), 595.

(14) O'Donnell, K.; Dierolf, V. *Rare-Earth Doped III-Nitrides for Optoelectronic and Spintronic Applications*; Springer: The Netherlands, 2010.

(15) Kenyon, A. J. Erbium in silicon. *Semicond. Sci. Technol.* **2005**, *20*, R65.

(16) Vinh, N. Q.; Przybylinska, H.; Krasil'nik, Z. F.; Gregorkiewicz, T. Microscopic structure of Er-related optically active centers in crystalline silicon. *Phys. Rev. Lett.* **2003**, *90* (6), 066401.

DOI: 10.1021/acsphotonics.7b01253
ACS Photonics 2018, 5, 1303−1309

(17) Vinh, N. Q.; Ha, N. N.; Gregorkiewicz, T. Photonic Properties of Er-Doped Crystalline Silicon. *Proc. IEEE* **2009**, *97*, 1269.
(18) Krasilnik, Z. F.; Andreev, B. A.; Kryzhkov, D. I.; Krasilnikova, L. V.; Kuznetsov, V. P.; Remizov, D. Y.; Shmagin, V. B.; Stepikhova, M. V.; Yablonskiy, A. N.; Gregorkievicz, T.; Vinh, N. Q.; Jantsch, W.; Przybylinska, H.; Timoshenko, V. Y.; Zhigunov, D. M. Erbium doped silicon single- and multilayer structures for light-emitting device and laser applications. *J. Mater. Res.* **2006**, *21* (3), 574−583.
(19) Favennec, P. N.; L'Haridon, H.; Salvi, M.; Moutonnet, D.; Leguillou, Y. Luminescence of Erbium Implanted in Various Semiconductors - IV-Materials, III-V-Materials and II-VI Materials. *Electron. Lett.* **1989**, *25* (11), 718.
(20) Feng, I. W.; Cao, X. K.; Li, J.; Lin, J. Y.; Jiang, H. X.; Sawaki, N.; Honda, Y.; Tanikawa, T.; Zavada, J. M. Photonic properties of erbium doped InGaN alloys grown on Si (001) substrates. *Appl. Phys. Lett.* **2011**, *98* (8), 081102.
(21) Feng, I. W.; Li, J.; Sedhain, A.; Lin, J. Y.; Jiang, H. X.; Zavada, J. Enhancing erbium emission by strain engineering in GaN hetero-epitaxial layers. *Appl. Phys. Lett.* **2010**, *96* (3), 031908.
(22) Ugolini, C.; Nepal, N.; Lin, J. Y.; Jiang, H. X.; Zavada, J. M. Erbium-doped GaN epilayers synthesized by metal-organic chemical vapor deposition. *Appl. Phys. Lett.* **2006**, *89*, 151903.
(23) George, D. K.; Hawkins, M. D.; McLaren, M.; Jiang, H. X.; Lin, J. Y.; Zavada, J. M.; Vinh, N. Q. Excitation mechanisms of Er optical centers in GaN epilayers. *Appl. Phys. Lett.* **2015**, *107* (17), 171105.
(24) Dahal, R.; Ugolini, C.; Lin, J. Y.; Jiang, H. X.; Zavada, J. M. 1.54 um emitters based on erbium doped InGaN p-i-n junctions. *Appl. Phys. Lett.* **2010**, *97* (14), 141109.
(25) Al Tahtamouni, T. M.; Stachowicz, M.; Li, J.; Lin, J. Y.; Jiang, H. X. Dramatic enhancement of 1.54 um emission in Er doped GaN quantum well structures. *Appl. Phys. Lett.* **2015**, *106* (12), 121106.
(26) Ramvall, P.; Tanaka, S.; Nomura, S.; Riblet, P.; Aoyagi, Y. Observation of confinement-dependent exciton binding energy of GaN quantum dots. *Appl. Phys. Lett.* **1998**, *73* (8), 1104.
(27) Look, D. C.; Sizelove, J. R. Predicted maximum mobility in bulk GaN. *Appl. Phys. Lett.* **2001**, *79* (8), 1133.
(28) Cao, Y.; Jena, D. High-mobility window for two-dimensional electron gases at ultrathin AlN/GaN heterojunctions. *Appl. Phys. Lett.* **2007**, *90* (18), 182112.
(29) Ho, V. X.; Dao, T. V.; Jiang, H. X.; Lin, J. Y.; Zavada, J. M.; McGill, S. A.; Vinh, N. Q. Photoluminescence quantum efficiency of Er optical centers in GaN epilayers. *Sci. Rep.* **2017**, *7*, 39997.
(30) Johnson, J. C.; Choi, H. J.; Knutsen, K. P.; Schaller, R. D.; Yang, P. D.; Saykally, R. J. Single gallium nitride nanowire lasers. *Nat. Mater.* **2002**, *1* (2), 106.
(31) Xing, G. C.; Mathews, N.; Lim, S. S.; Yantara, N.; Liu, X. F.; Sabba, D.; Gratzel, M.; Mhaisalkar, S.; Sum, T. C. Low-temperature solution-processed wavelength-tunable perovskites for lasing. *Nat. Mater.* **2014**, *13* (5), 476.
(32) Coldren, L. A.; Corzine, S. W. *Diode Lasers and Photonic Integrated Circuits*; Wiley: New York, 1995.
(33) Wu, S. F.; Buckley, S.; Schaibley, J. R.; Feng, L. F.; Yan, J. Q.; Mandrus, D. G.; Hatami, F.; Yao, W.; Vuckovic, J.; Majumdar, A.; Xu, X. D. Monolayer semiconductor nanocavity lasers with ultralow thresholds. *Nature* **2015**, *520* (7545), 69.
(34) Tessler, N. Lasers based on semiconducting organic materials. *Adv. Mater.* **1999**, *11* (5), 363.
(35) Shaklee, K. L.; Leheny, R. F. Direct Determination of Optical Gain in Semiconductor Crystals. *Appl. Phys. Lett.* **1971**, *18* (11), 475.

DOI: 10.1021/acsphotonics.7b01253
ACS Photonics 2018, 5, 1303−1309